Defective GABAergic neurotransmission in the nucleus tractus solitarius in *Mecp2*-null mice, a model of Rett syndrome

Chao-Yin Chen (陳昭吟)[a],[*], Jacopo Di Lucente[b], Yen-Chu Lin[b], Cheng-Chang Lien[e],
Michael A. Rogawski[c], Izumi Maezawa[b,d], Lee-Way Jin[b,d,**]

[a] *Department of Pharmacology, University of California Davis, One Shields Avenue, Davis, CA 95616, United States*
[b] *Department of Pathology and Laboratory Medicine, University of California Davis, One Shields Avenue, Davis, CA 95616, United States*
[c] *Department of Neurology, University of California Davis, One Shields Avenue, Davis, CA 95616, United States*
[d] *M.I.N.D. (Medical Investigation of Neurodevelopmental Disorders) Institute, University of California Davis, One Shields Avenue, Davis, CA 95616, United States*
[e] *Institute of Neuroscience, National Yang-Ming University, Taipei 112, Taiwan*

ARTICLE INFO

ABSTRACT

Rett syndrome (RTT) is a devastating neurodevelopmental disorder caused by loss-of-function mutations in the X-linked methyl-CpG binding protein 2 (*Mecp2*) gene. GABAergic dysfunction has been implicated contributing to the respiratory dysfunction, one major clinical feature of RTT. The nucleus tractus solitarius (NTS) is the first central site integrating respiratory sensory information that can change the nature of the reflex output. We hypothesized that deficiency in *Mecp2* gene reduces GABAergic neurotransmission in the NTS. Using whole-cell patch-clamp recordings in NTS slices, we measured spontaneous inhibitory postsynaptic currents (sIPSCs), miniature IPSCs (mIPSCs), NTS-evoked IPSCs (eIPSCs), and GABA$_A$ receptor (GABA$_A$-R) agonist-induced responses. Compared to those from wild-type mice, NTS neurons from *Mecp2*-null mice had significantly ($p < 0.05$) reduced sIPSC amplitude, sIPSC frequency, and mIPSC amplitude but not mIPSC frequency. *Mecp2*-null mice also had decreased eIPSC amplitude with no change in paired-pulse ratio. The data suggest reduced synaptic receptor-mediated phasic GABA transmission in *Mecp2*-null mice. In contrast, muscimol (GABA$_A$-R agonist, 0.3–100 μM) and THIP (selective extrasynaptic GABA$_A$-R agonist, 5 μM) induced significantly greater current response in *Mecp2*-null mice, suggesting increased extrasynaptic receptors. Using qPCR, we found a 2.5 fold increase in the delta subunit of the GABA$_A$-Rs in the NTS in *Mecp2*-null mice, consistent with increased extrasynaptic receptors. As the NTS was recently found required for respiratory pathology in RTT, our results provide a mechanism for NTS dysfunction which involves shifting the balance of synaptic/extrasynaptic receptors in favor of extrasynaptic site, providing a target for boosting GABAergic inhibition in RTT.

1. Introduction

Rett syndrome (RTT), caused by loss-of-function mutations in the X-linked gene encoding the epigenetic regulator *Mecp2* (methyl-CpG-binding protein 2), is a devastating neurodevelopmental disorder that primarily affects young girls (Ellaway and Christodoulou, 1999; Chahrour and Zoghbi, 2007). Although it is a rare disorder, RTT has recently become a prototypical model for studying synaptic dysfunction in neurological disorders (Chahrour and Zoghbi, 2007). RTT is also categorized as a syndromic autism spectrum disorder and shares important pathogenic pathways with autism (Levitt and Campbell, 2009; Gonzales and LaSalle, 2010). A major cause of morbidity and mortality in RTT is dysfunctional respiratory control due to *Mecp2* deficiency

(Katz et al., 2009). Conclusions from genetic, neurochemical, and pharmacological studies support that depressed GABAergic neurotransmission in the brainstem contributes to RTT breathing abnormalities (Chao et al., 2010; Ure et al., 2016). Augmenting GABAergic neurotransmission has been shown to improve the respiratory phenotype in RTT mouse models and to prolong survival (Abdala et al., 2010; Voituron and Hilaire, 2011; Bittolo et al., 2016).

Respiratory neurons reside mainly in two regions of the brainstem: the dorsal respiratory group in the nucleus tractus solitaries (NTS) and the ventral respiratory group in the ventrolateral medulla (Bonham, 1995). Glutamate is the main excitatory neurotransmitter involved in the central generation of respiratory rhythm while GABA acting on GABA$_A$ receptors (GABA$_A$-Rs) provides phasic waves of inhibition to

---

shape the pattern of the respiratory motor output (Bonham, 1995). Wasserman and colleagues showed that blocking GABA reuptake with nipecotic acid in the NTS increased inspiratory duration that frequently culminates in apneustic breathing (Wasserman et al., 2002). They further showed that $GABA_B$ receptors mediated the increased inspiratory duration and $GABA_A$-Rs mediated the apnea effects. Importantly, in *Mecp2*-null mice, selective recovery of *Mecp2* expression in the HoxA4 domain, which includes caudal parts of NTS and ventral respiratory column, was sufficient to restore normal respiratory rhythm and prevent apnea (Huang et al., 2016), suggesting an important role of the NTS in RTT pathophysiology. Thus, we focused on NTS $GABA_A$-R dysfunction in a *Mecp2-null* mouse model in order to provide a pathophysiological basis for abnormal respiratory regulation in RTT.

2. Materials and methods

2.1. Mouse model of RTT

All experimental protocols were carried out with approval from the Institutional Animal Care and Use Committee of the University of California Davis. $Mecp2^{tm1.1Bird/+}$ mice, which originated from Dr. Adrian Bird's laboratory (Guy et al., 2001), were obtained from Jackson Laboratories (Bar Harbor, Maine). Mice were mated with C57BL/6 J mice (Jackson Laboratories). Mice were genotyped to determine the *Mecp2* deletion according to the protocol provided by the Jackson Laboratory. The *Mecp2*-null males 7 to 10 weeks old were used in the present study as a mouse model of RTT, while their male littermates served as the WT control. The sex of the pups was determined using primers for the *Sry* gene on Y chromosome, which were 5′-TGG GAC TGG TGA CAA TTG TC-3′ and 5′-GAG TAC AGG TGT GCA GCT CT-3′.

2.2. Whole-cell patch-clamp recordings

Brain slices containing the NTS were obtained as previously described (Chen et al., 2009; Sekizawa et al., 2012, 2013). The mice were anesthetized with isoflurane and decapitated. The brain was rapidly removed and submerged in ice-cold ($< 4 \, ^\circ C$) high-sucrose artificial cerebrospinal fluid (aCSF) that contained (mM): 3 KCl, 2 $MgCl_2$, 1.25 NaH_2PO_4, 26 $NaHCO_3$, 10 glucose, 220 sucrose and 2 $CaCl_2$, pH 7.4 when continuously bubbled with 95% O_2/5% CO_2. Brainstem transverse slices (250 μm thick) were cut with the Vibratome 1000 (Technical Products International, St. Louis, MO). After incubation for 45 min at 35 °C in high-sucrose aCSF, the slices were placed in normal aCSF that contained (mM): 125 NaCl, 2.5 KCl, 1 $MgCl_2$, 1.25 NaH_2PO_4, 25 $NaHCO_3$, 10 glucose and 2 $CaCl_2$, pH 7.4 when continuously bubbled with 95% O_2/5% CO_2. During the experiments a single slice was transferred to the recording chamber, held in place with a nylon mesh, and continuously perfused with oxygenated aCSF at a rate of ~ 3 ml/min. Borosilicate glass electrodes (BF150-86-10, Sutter Instrumnt, Novato, CA) were filled with a CsCl solution containing (in mM): 140 CsCl, 5 NaCl, 1 $MgCl_2$, 3 K-ATP, 0.2 Na-GTP, 10 EGTA, 10 HEPES, and 5 QX314. The pH was adjusted to 7.3 with CsOH. The seal resistance was > 1 GΩ. The series resistance was no > 15 MΩ and not different (t-test, $p > 0.05$) between wild type (13.2 ± 0.5 MΩ, mean ± SEM) and *Mecp2*-null (13.6 ± 0.6 MΩ, mean ± SEM) mice. Recordings were made with a MultiClamp 700B patch-clamp amplifier (Molecular Devices, Sunnyvale, CA). Whole-cell currents were filtered at 2 kHz and digitized at 10 kHz with a DigiData 1440A interface (Molecular Devices).

The neurons were voltage clamped at -60 mV. All experiments were performed in the presence of ionotropic glutamate receptor antagonists, 1,2,3,4-tetrahydro-6-nitro-2,3-dioxo-benzo[f]quinoxaline-7-sulfonamide disodium salt (NBQX, 10 μM) and DL-2-amino-5-phosphonopentanoic acid (AP-5, 50 μM) to isolate the inhibitory currents from excitatory currents.

To determine the inhibitory synaptic input, spontaneous inhibitory postsynaptic currents (sIPSCs) were recorded for 6 min. The sIPSCs in the last 3 min of the recording were used for data analysis. To isolate the action potential-independent synaptic inputs, miniature IPSCs (mIPSCs) were recorded in the presence of the sodium channel blocker, tetrodotoxin (TTX, 1 μM). To stimulate GABA release from local inhibitory neurons in the NTS for evoked-IPSCs (eIPSCs), a bipolar tungsten electrode (1 μm tips separated by 80 μm) was placed in the intermediate NTS ipsilateral and medial to the recording site. We used the minimal intensity (4–8 V, 0.1 ms duration) required to consistently evoke IPSCs. There was no difference (t-test, $p > 0.05$) in the intensities used to evoke IPSCs in WT (6.6 ± 0.3 V, mean ± SEM) and *Mecp2*-null mice (6.7 ± 0.4 V, mean ± SEM). The averaged distance between the stimulating electrode and the recorded neurons was 361 ± 5.71 μm (mean ± SEM; ranging from 300 μm to 420 μm). Pairs of NTS stimuli with an inter-pulse interval of 60 ms were delivered at 0.1 Hz to determine paired-pulse ratios (Chen and Bonham, 2005). In separate neurons, muscimol (30 s perfusion, 0.3–100 μM)- or THIP (5 μM)-induced whole-cell currents were recorded. $GABA_A R$ agonist, muscimol, was applied in the bath for 30 s, after a stable baseline was recorded. To evaluate changes in GABAergic tonic current, 10 min were allowed in order for the response to stabilize, and the recorded baseline activity for approximately 3 min follow by the bath perfusion for 4 min of the $GABA_A R$ partial agonist THIP (5 μM) to increase GABAergic tonic current. After THIP perfusion, $GABA_A R$ antagonist bicuculline (30 μM) was added to block both phasic and tonic currents. To confirm that the recorded currents were IPSCs and agonist-induced whole cell currents were recorded before and after perfusion with the $GABA_A$-R antagonist bicuculline (30 μM) in some neurons.

2.3. Quantitative PCR (qPCR)

Brainstem slices (300 μm) containing the NTS were obtained as described above. Bilateral punches of the NTS were obtained with a 0.5 mm biopsy punch (World Precision Instruments, Sarasota, FL). RNA was extracted using an RNeasy Plus Mini Kit (Qiagen, Valencia, CA), according to the manufacturer's protocol. cDNA was synthesized using iScript Reverse Transcription Supermix (Bio-Rad, Hercules, CA). RNA purity and concentrations were assessed by measuring the absorbance at 260 nm, and 280 nm using a NanoDrop 2000C Spectrophotometer (Thermo Scientific, Waltham, MA). Quantitative PCR (qPCR) was performed using the SsoFast EvaGreen Supermix (Bio-Rad, Hercules, CA) in the CFX96 Touch Real-Time PCR Detection System (Bio-Rad). The primer sequences used to quantify $GABA_A$-R subunit mRNAs are listed in Table 1. For β-actin, we used the commercially available primer set Mouse ACTB (Actin, Beta) Endogenous Control FAM Dye/MGB Probe, Non-Primer Limited (Invitrogen, Carlsbad, CA). Gene expression was normalized to an endogenous reference gene, β-actin. Data were analyzed with the 2-ΔCt method. All experiments were performed in duplicate.

2.4. Statistical analysis

The sIPSC and mIPSC events were detected with MiniAnalysis software (Synaptosoft, Fort Lee, NJ). The accuracy of detection was confirmed by visual inspection. Data are expressed as means ± SEM. Statistical analyses were performed using SigmaPlot software (Systat Software, Inc., San Jose, CA). A t-test was used to compare between wild type and *Mecp2*-null mice for the following measurements: sIPSC/mIPSC frequency and amplitude, eIPSC amplitude, decay time constant, and paired-pulse ratio. A two-way repeated ANOVA was used to compare THIP- and muscimol-induced responses, followed by Fisher's LSD test for pairwise comparison when appropriate. Relative cDNA levels for the target genes were analyzed by the 2-ΔΔCt method using Actb (β-actin) as the internal control for normalization (Livak and Schmittgen, 2001). A t-test was used to compare between WT and *Mecp2*-null mice. A p value of < 0.05 was considered statistically significant.

Table 1
Primer sequences.

Gene	Forward primer (5′ → 3′)	Reverse primer (3′ → 5′)
α1	GAGCACACTGTCGGGAGGAA	GCTCTCCCAAACCTGGTCTC
α2	TGACTCCGTTCAGGTTGCTC	TGCAAGGCAGATAGGTCTGA
α3	CTCTCTGCTTCGGGGAAGTG	ATTCCCCTTGGCTAGTGGTT
α4	AGTCAGTGGAGGTGCCAAAG	GGTGGTCATCGTGAGGACTG
α5	CCCCTGAAATTTGGCAGTAT	CAGGTGGAAGTGAGCAGTCA
α6	GACTTTGCCCATCGTTCC	TGCAAAAGCTACTGGGAAGAG
β1	GGTTTGTTGTGCACACAGCTCC	ATGCTGGCGACATCGATCCGC
β2	GCTGGTGAGGAAATCTCGGTCCC	CATGCGGCACGGCGTACCAAA
β3	GAGCGTAAACGACCCCGGGAA	GGGACCCCCGAAGTCGGGTCT
γ1	ATCCACTCTCATTCCCATGAACAGC	ACAGAAAAAGCTAGTACAGTCTTTGC
γ2	ACTTCTGGTGACTATGTGGTGAT	GGCAGGAACAGCATCCTTATTG
γ3	ATTACATCCAGATTCCACAAGATG	CACAGGTGTCCTCAAATTCCT
δ	TGGCCAGCATTGACCATATC	CCAGCTCTGATGCAGGAACA

2.5. Chemicals

Isoflurane was obtained from Piramal (Bethlehem, PA). QX 314 was obtained from Tocris Bioscience (Bristol, United Kingdom). TTX, bicuculline, NBQX, and AP-5 were obtained from Sigma-Aldrich (St. Louis, MO). All other chemicals were obtained from Fisher Scientific (Hampton, NH). Reverse Transcription Supermix, and SsoFast EvaGreen Supermix were obtained from Bio-Rad (Hercules, CA).

3. Results

Whole-cell patch-clamp data were obtained from 67 neurons in 28 wild type (WT) mice and 63 neurons in 24 *Mecp2*-null mice. There was no difference (*t*-test, $p > 0.05$) in cell capacitance (17.9 ± 1.5 pF vs. 18.5 ± 1.1 pF, wild type vs. *Mecp2*-null, respectively). There was also no difference (*t*-test, $p > 0.05$) in whole cell input resistance (698 ± 42 MΩ vs. 660 ± 51 MΩ, wild type vs. *Mecp2*-null, respectively).

3.1. Reduced sIPSC amplitude and frequency in NTS neurons in Mecp2-null mice

Example recordings of sIPSCs from the NTS neurons are shown in Fig. 1A. The group data of *Mecp2*-null neurons, compared to WT neurons, showed a leftward shift in the cumulative probability of the sIPSC amplitude (Fig. 1B, left) with a rightward shift in the inter-event intervals (Fig. 1B, right). The mean sIPSC amplitude (Fig. 1C, left) was significantly lower (*t*-test, $p < 0.05$) in *Mecp2*-null mice than that in WT mice. The mean frequency (Fig. 1C, right) was also significantly lower (*t*-test, $p < 0.05$) in *Mecp2*-null mice than that in WT mice. There was no significant difference (*t*-test, $p > 0.05$) in IPSC decay time (19 ± 1 ms vs. 21 ± 2 ms, WT vs. *Mecp2*-null, respectively). The data suggest that *Mecp2*-null mice had reduced synaptically-mediated phasic inhibitory inputs in the NTS.

3.2. Reduced mIPSC amplitude but not frequency in Mecp2-null mice

The reduced sIPSC frequency could be mediated by changes in the action potential-mediated neurotransmitter release and/or action potential-independent release. We recorded mIPSCs in the presence of TTX (1 μM) to eliminate action potential-dependent synaptic events. Fig. 2 shows example recordings of mIPSCs from NTS neurons. Similar to sIPSCs, the group data of *Mecp2*-null neurons, compared to WT neurons, showed a leftward shift in the cumulative probability of the mIPSC amplitude (Fig. 2B, left). However, in contrast to sIPSCs, there was no difference in the cumulative probability of the inter-event interval (Fig. 2B, right). The mean mIPSC amplitude (Fig. 2C, left) was significantly lower (*t*-test, $p < 0.05$) in *Mecp2*-null mice than that in WT mice. The mean frequency (Fig. 2C, right) was not different

between WT and *Mecp2*-null mice. There was also no difference (*t*-test, $p > 0.05$) in decay time (22 ± 2 ms vs. 23 ± 1 ms, wild type vs. *Mecp2*-null, respectively). These mIPSC events were completely blocked by 30 μM of bicuculline (data not shown), confirming that these are GABA$_A$-R mediated synaptic events. Together, our sIPSC and mIPSC data suggest that 1) the reduced sIPSC event frequency was due to reduced action potential-dependent GABA release (reduced activity of GABAergic interneurons); and 2) *Mecp2*-null mice had reduced phasic synaptic GABAergic transmission in the NTS.

3.3. Reduced eIPSC amplitudes but not the paired-pulse ratio (PPR) in Mecp2-null mice

As shown in Fig. 3A & B the NTS-evoked IPSC amplitude was significantly smaller in neurons from *Mecp2*-null mice. The time courses of eIPSCs from both groups appear to be similar after scaling the IPSCs to the same peak amplitude (Fig. 3A, right). There was no difference (*t*-test, $p > 0.05$) in decay time constants (21.6 ± 2.6 ms vs. 23.5 ± 2.8 ms, wild type vs. *Mecp2*-null, respectively). The reduced eIPSC amplitude was not associated with a change in the PPR (60 ms interval, Fig. 3C, D). The data suggest that the reduced phasic synaptic inhibition is likely mediated by postsynaptic mechanism(s) and not a change in presynaptic release probability.

3.4. Enhanced GABA$_A$-R agonist-induced currents in Mecp2-null mice

In the presence of NBQX, AP-5, and TTX, exogenous application of a GABA$_A$-R agonist, muscimol, induces concentration-dependent inward currents. Fig. 4A shows example traces of muscimol-induced currents from one WT and one *Mecp2*-null mouse. Interestingly, in contrast to reduced phasic synaptic transmission, the amplitudes of muscimol-induced currents were larger in the *Mecp2*-null mouse. The group data (Fig. 4B) confirmed that *Mecp2*-null mice had a significantly greater response to GABA$_A$-R activation with muscimol (two-way ANOVA: $p < 0.05$, genotype; $p < 0.05$, concentration; $p < 0.05$, interaction).

Given that exogenous application of the GABA$_A$-R agonist activated both synaptic and extrasynaptic GABA$_A$-Rs, we tested the agonist-induced response with THIP, a selective extrasynaptic GABA$_A$-R agonist. Fig. 5A shows example traces of whole cell current response to application of THIP (5 μM) in the absence and presence of bicuculline (30 μM). Example traces show that THIP induced a greater inward current in the neuron from the *Mecp2*-null mouse. Bicuculline blocked the THIP-induced currents, in addition to blocking phasic synaptic events, indicating that the THIP-induced currents were mediated by GABA$_A$-Rs. The group data confirmed that THIP-induced a greater current in *Mecp2*-null mice (Fig. 5B, left) and bicuculline blocked the THIP-induced current in both WT and *Mecp2*-null mice (two-way ANOVA: $p < 0.05$, genotype; $p < 0.05$, concentration; $p < 0.05$, interaction). THIP also significantly increased the noise variance in
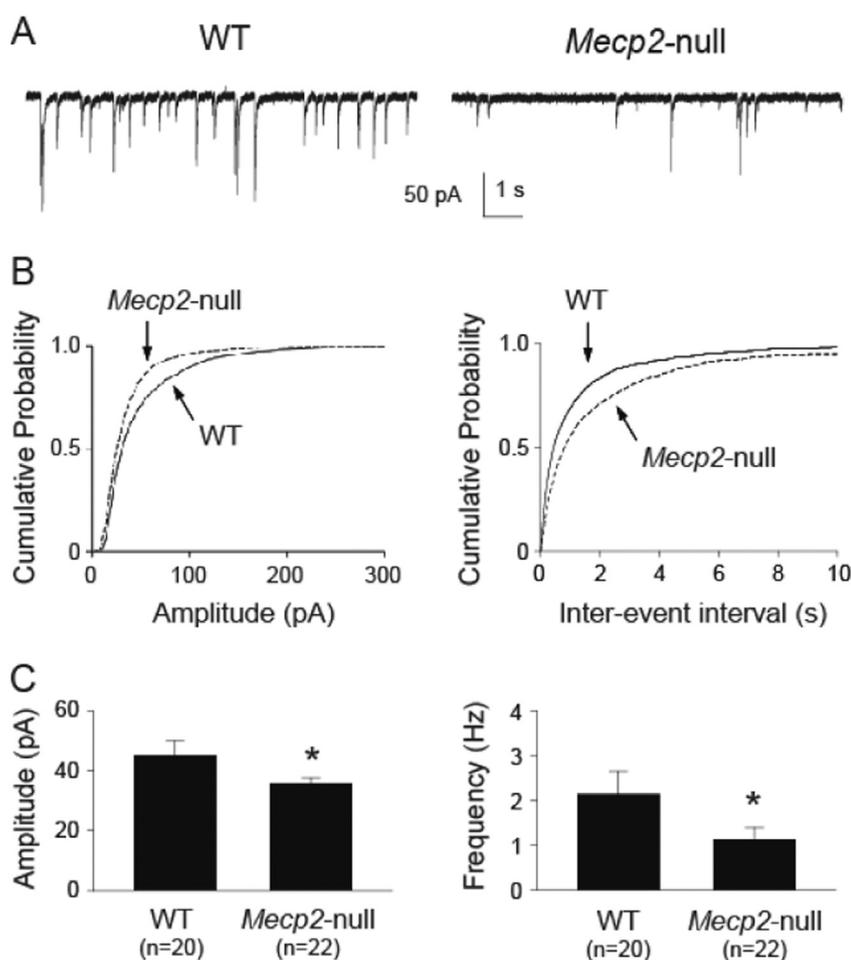
Fig. 1. *Mecp2*-null mice had reduced sIPSC amplitude and frequency in the NTS. A. Example traces of sIPSC recorded from one wild type (WT) and one *Mecp2*-null mouse. B. Cumulative probability plot from all recorded neurons showing a leftward shift in sIPSC amplitude (left), suggesting reduced sIPSC amplitude in *Mecp2*-null mice. There was a rightward shift in inter-event interval cumulative plot (right), suggesting a reduction in sIPSC frequency. C. Group data showing reduced mean sIPSC amplitude (left) and frequency (right). *, $p < 0.05$ *Mecp2*-null vs. WT (*t*-test).

both groups (Fig. 5B right, two-way ANOVA: $p > 0.05$, genotype; $p < 0.05$, concentration; $p < 0.05$, interaction). The increase in the noise variance was significantly greater (*t*-test, $p < 0.05$) in the *Mecp2*-null mice (3.8 ± 0.7 vs. 6.1 ± 1.2, WT vs. *Mecp2*-null, respectively). The data suggest an increase in extrasynaptic GABA$_A$-R function in the *Mecp2*-null mice. Furthermore, bicuculline significantly reduced the noise variance (compared to the baseline) in *Mecp2*-null mice but not in WT mice, suggesting an elevated tonic extrasynaptic GABA$_A$-R function in *Mecp2*-null mice.

3.5. Differential expression of GABA$_A$-R subunit transcripts in Mecp2-null mice

The subunit compositions of extrasynaptic GABA$_A$-Rs are different from those of synaptic GABA$_A$-Rs. Because deficiency of *Mecp2*, functioning as an epigenetic modulator, changes cellular transcriptomic landscape (Pohodich and Zoghbi, 2015), we hypothesized altered NTS gene expression in RTT shifting toward extrasynaptic GABA$_A$-R subunits. Fig. 6 shows the transcript levels of NTS GABA$_A$-R subunits of *Mecp2*-null mice, expressed as fold change from those of WT mice. *Mecp2*-null NTS had significantly lower α4 and α5 subunits (*t*-test, $p < 0.05$). Importantly, all three γ subunits were significantly reduced while the δ subunit, found exclusively in extrasynaptic site, increased by > 2 folds (*t*-test, $p < 0.05$). The data are consistent with the electrophysiology data showing an increase in extrasynaptic GABA$_A$-R function and suggest that there is a shift in GABA$_A$-Rs from synaptic to extrasynaptic site in *Mecp2*-null mice.

4. Discussion

In this study, we sought to identify anatomy- and physiology-informed GABAergic mechanisms leading to dysfunctional respiratory control in RTT. We focused on the NTS, a medulla nucleus containing gateway synapses that integrate sensory input to coordinate reflex output of respiratory control (Andresen and Kunze, 1994; Joad et al., 2004; Bonham et al., 2006a, 2006b). We found reduced sIPSC and mIPSC amplitudes in NTS neurons in *Mecp2*-null mice, suggesting reduced phasic synaptic GABAergic transmission. Spontaneous IPSC frequency, but not mIPSC frequency, was reduced in *Mecp2*-null mice, reflecting a general reduction of the activity of GABAergic neurons. Because eIPSC amplitude was also reduced in the *Mecp2*-null NTS neurons, but there was no changes in PPR, we concluded that the reduced GABAergic neurotransmission was mainly due to postsynaptic mechanism(s). Interestingly, despite this postsynaptic deficit, *Mecp2*-null neurons showed enhanced responses to muscimol, which activates both synaptic and extrasynaptic GABA$_A$-Rs, and THIP, which selectively activates extrasynaptic GABA$_A$-Rs. These results, together with the altered gene expression pattern of GABA$_A$-R subunits (significant reductions of all three γ subunits and a more than two fold increase of the δ subunit) in the *Mecp2*-null NTS, suggest a shift in GABA$_A$-Rs from synaptic to extrasynaptic loci. Taken together, our data suggest that NTS GABAergic dysfunction in RTT is mainly due to postsynaptic mechanisms that may involve an imbalance between phasic (synaptic) and tonic (extrasynaptic) inhibitory tones. Moreover, there is reduced GABA release due to reduced GABAergic neuronal activities, but not due to reduced presynaptic GABA release probability.

Our results complement the finding of Kline et al. (2010), who studied EPSCs in the NTS, although they used the *Mecp2$^{tm1-1Jae}$* model
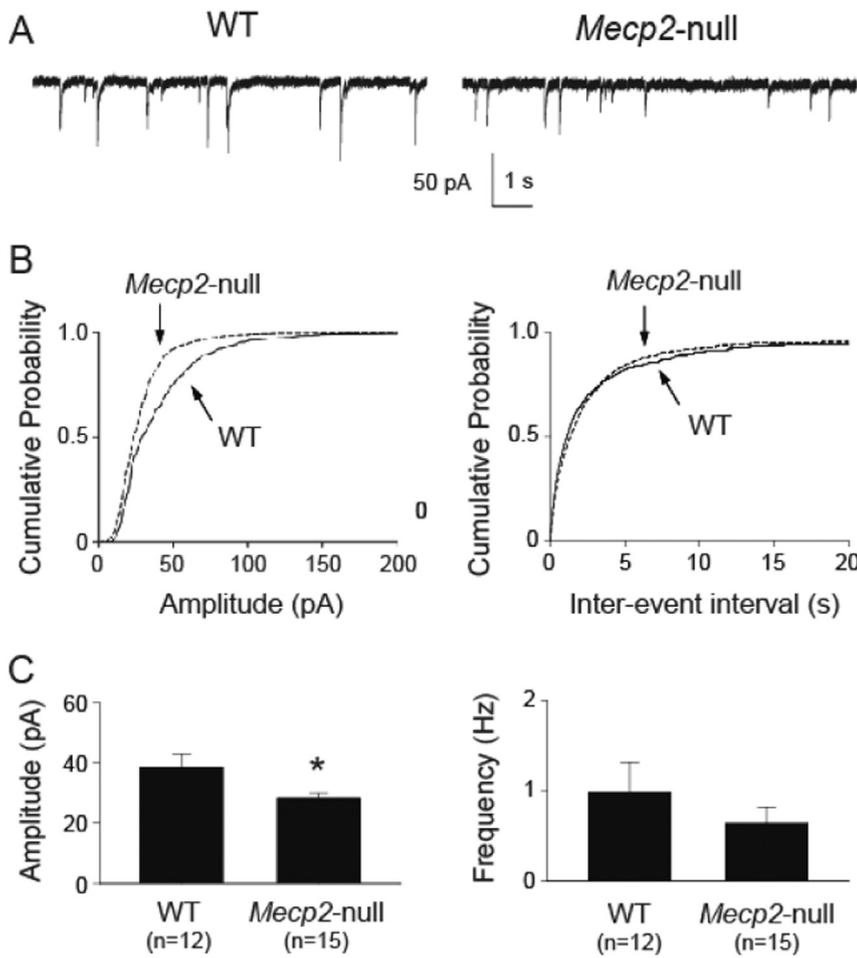
Fig. 2. *Mecp2*-null mice had reduced mIPSC amplitude but not frequency in the NTS. A. Example traces of mIPSC recorded from one wild type (WT) and one *Mecp2*-null mouse. B. Cumulative probability plot from all recorded neurons showing a leftward shift in mIPSC amplitude (left), suggesting reduced sIPSC amplitude in *Mecp2*-null mice. There was no difference in inter-event interval cumulative plot (right). C. Group data showing reduced mean sIPSC amplitude (left) but not frequency (right). *, $p < 0.05$ *Mecp2*-null vs. WT (*t*-test).
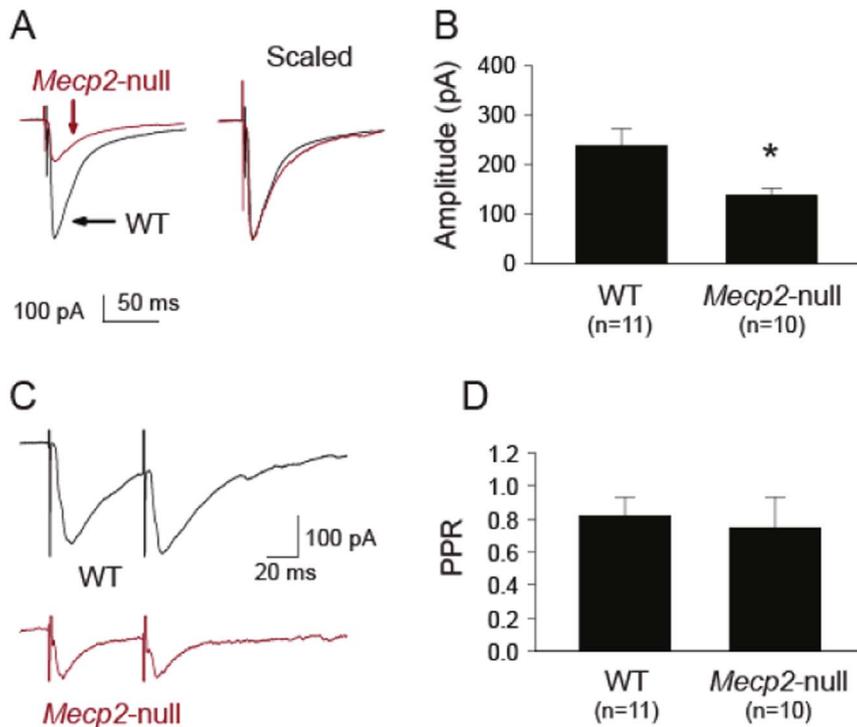

Fig. 3. *Mecp2*-null mice had reduced eIPSC amplitude but not paired-pulse ratio in the NTS. A. Example traces of NTS-evoked IPCSs from one WT and one *Mecp2*-null mouse. Left, traces shown as their relative amplitude; right, traces scaled to the same peak amplitude. B. Group data showing that the eIPSC amplitude was significantly smaller in neurons from the *Mecp2*-null mice. C. Example traces of NTS-evoked paired IPSCs from one WT and one *Mecp2*-null mouse. D. Group data showing similar paired-pulse ratio (60 ms inter stimulus interval) between the two groups, suggesting a postsynaptic mechanism mediating the reduced IPSC amplitude in *Mecp2*-null mice. *, $p < 0.05$ *Mecp2*-null vs. WT (*t*-test).
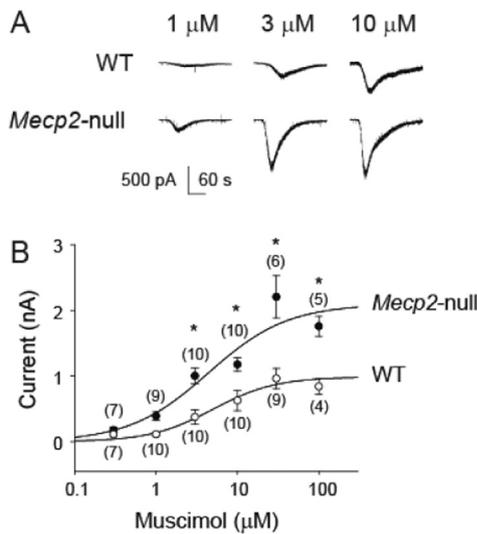
Fig. 4. *Mecp2*-null mice had larger muscimol-induced currents in the NTS. A. Example traces of muscimol-induced concentration-dependent current responses from one WT and one *Mecp2*-null mouse. Black bar indicates application of muscimol. B. Group data of concentration-dependent response showing enhanced muscimol-induced currents in neurons recorded from the *Mecp2*-null mice (two-way ANOVA: $p < 0.05$, genotype; $p < 0.05$, concentration; $p < 0.05$, interaction). Numbers in parentheses indicate number of neurons. *, $p < 0.05$, *Mecp2*-null vs. FA, Fisher's LSD *post-hoc* test.

(Chen et al., 2001), which differs from the complete knockout *Mecp2*$^{tm1.1Bir}$ model used in our study in that the *Mecp2*$^{tm1-1Jae}$ allele still produces a truncated and modified protein product. They found that the amplitudes of spontaneous, miniature, and evoked EPSCs in NTS neurons were all significantly increased in *Mecp2*$^{tm1-1Jae/Y}$ mice. This was unaffected by blockade of inhibitory GABA currents, suggesting independent *Mecp2*-regulated mechanisms enhancing the excitatory tones. Together, the data suggest that there is a shift in the balance of excitation and inhibition toward excitatory tone in the NTS.

Overall, the consequence of *Mecp2* deficiency appears to be an aggravated imbalance between synaptic excitation and inhibition (Dani
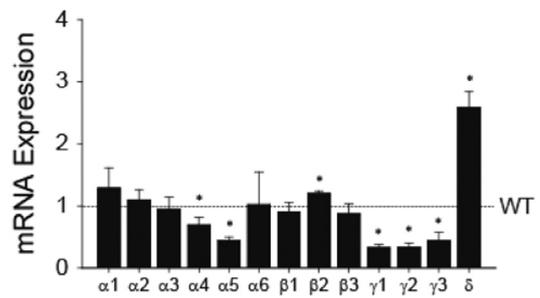

Fig. 6. GABA$_A$-R subunit mRNA expression level in the NTS. All data were normalized to expression level of the WT (dotted line). N = 4 in each group. *, $p < 0.05$ vs. WT (t-test on data before normalizing to WT).

et al., 2005; Chao et al., 2007; Medrihan et al., 2008; Zhang et al., 2008; Chao et al., 2010; Banerjee et al., 2016). The notion of pathological disruption of excitatory/inhibitory homeostasis resulting in behavior symptoms in RTT is further supported by studies of mouse models with selective knockout of *Mecp2* in glutamatergic neurons (Meng et al., 2016), GABAergic neurons (Chao et al., 2010; Banerjee et al., 2016), or selective rescue of GABA/glycine inhibitory neurons (Ure et al., 2016). In the NTS, this shift in synaptic excitability toward excitation could contribute to altered respiratory regulation in RTT, including apneustic breathing (Bonham, 1995; Burton and Kazemi, 2000).

Although changes in excitatory and inhibitory transmissions are commonly detected in RTT, the specific changes appear to be age- and brain region-dependent, perhaps not surprisingly given the time-dependent progression of the disease and functions of different brain regions. For example, Medrihan et al. showed that, in neonates (p7), there was an increased excitatory transmission coupled with a reduction in the number of GABA synapses in ventrolateral medulla, an area of the reticular brain stem formation including the pre-Bötzinger complex responsible for generating the respiratory rhythm (Medrihan et al., 2008). Abdala et al. showed reduced GABAergic terminal projections in the Kölliker–Fuse nucleus in the dorsolateral pons, and administration of a drug that augments endogenous GABA localized to this region reduced the incidence of apnea and the respiratory irregularity of RTT
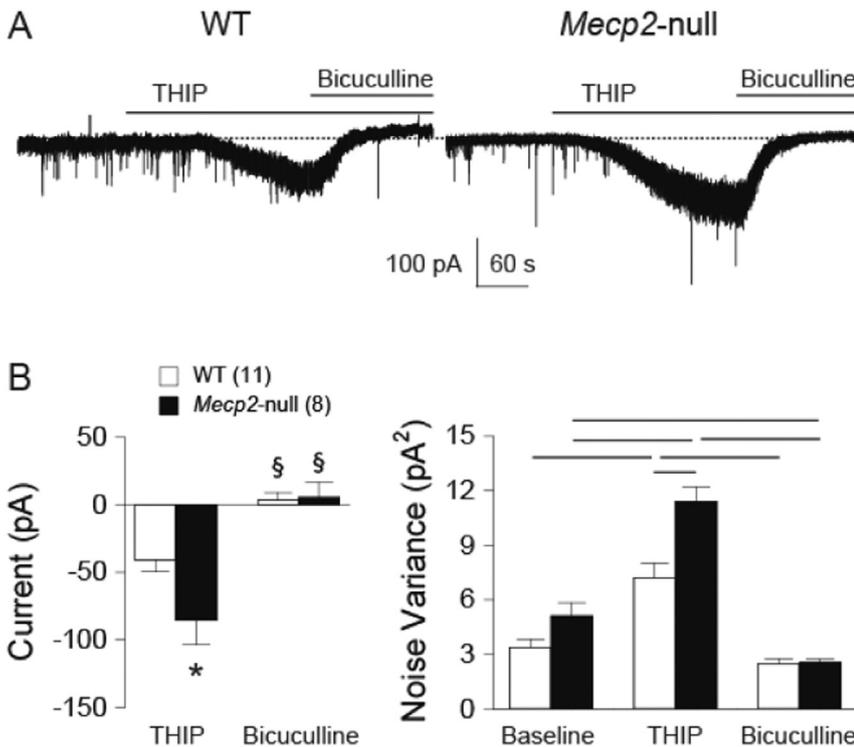

Fig. 5. *Mecp2*-null mice had larger THIP-induced currents in the NTS. A. Example traces of THIP-induced current responses before and during bicuculline perfusion from one WT and one *Mecp2*-null mouse. B. Group data of changes in current from baseline (before THIP application) showing enhanced THIP-induced currents in neurons recorded from the *Mecp2*-null mice (Fisher's LSD *post-hoc* test: *, $p < 0.05$ WT vs. *Mecp2*-null; §, $p < 0.05$ THIP vs. Bicuculline within the same genotype). C. Group data of noise variance before THIP application (Baseline), during THIP, and during THIP + bicuculline (bicuculline). THIP significantly increased noise variance in both groups. Each line on top indicates $p < 0.05$ between the two bars, Fisher's LSD *post-hoc* test.

female mice (Abdala et al., 2016). In contrast, our data suggest that NTS neurons in *Mecp2*-null mice have reduced phasic GABA transmission mainly due to postsynaptic receptor mechanism(s). Similarly, Jin and colleagues showed a reduction in sIPSC frequency and amplitude – but not before the age of 3 weeks in locus coeruleus (LC), a pontine nucleus that provide major norepinephrine projections (Jin et al., 2013).

In addition to changes in reduction in phasic synaptic transmission, we detected an increase in the extrasynaptic $GABA_A$-R that was not seen in p7 in Medrihan's study, suggesting that enhanced tonic inhibition maybe a beneficial mechanism to compensate for the falling phasic GABAergic neurotransmission. Parallel to our finding in the NTS, Jiang and colleagues showed augmentations of tonic currents and noise variance by THIP in LC neurons, with a greater degree of increase in *Mecp2*-null neurons than in WT neurons (Zhong et al., 2015). Also similar to our findings in the NTS, they found, in the LC, a reduction in the expression of $GABA_A$-R α5 subunit and a close to two fold increase in δ, the major subunit component of extrasynaptic $GABA_A$-Rs (Nusser et al., 1998). The changes in subunit expression may contribute to enhanced tonic GABA currents in *Mecp2*-null neurons. We further found that all three γ subunits were significantly reduced in *Mecp2*-null NTS neurons; among which γ2 is well-known to be involved in direct GABAergic synaptic transmission (Farrant and Nusser, 2005).

The variations of reported GABAergic deficits in different brainstem nuclei suggest that local dynamics of *Mecp2*-regulated $GABA_A$-R subunit expression may contribute to various reorganizations and synaptic/extrasynaptic distributions of $GABA_A$-R variants, a mechanism requiring further studies. First, alterations in the tonic $GABA_A$-R-mediated conductance have been implicated in disruptions in network dynamics associated with some neurological disorders (Brickley and Mody, 2012). Is enhanced tonic inhibition truly a beneficial compensatory mechanism or is it aggravating the network dysfunction underlying seizure and respiratory dysfunction in RTT? Second, the NTS receives and integrates sensory afferents from multiple tissues, including those carrying information about blood pressure. Does the enhanced tonic inhibition in the NTS alter other autonomic functions such as blood pressure regulation? Third, the observation of enhanced tonic inhibition in at least two distinct brainstem structures (NTS and LC) could be therapeutically significant. Is it generalizable beyond the two brainstem nuclei? Such questions are highly important as enhancement of GABAergic neurotransmission is currently considered a promising therapy for RTT but approaches for effective long-term GABAergic inhibition remain to be found. If tonic inhibition is beneficial, the effect can be augmented by compounds selectively enhancing the tonic inhibition, which in principle will work well since our data show that extrasynaptic $GABA_A$-R species underlying tonic inhibition appear to be over-expressed and active in RTT. In this regard, Zhong et al. showed that early-life exposure of *Mecp2*-null mice to THIP alleviated breathing abnormalities (Zhong et al., 2016), suggesting that enhancing tonic inhibition could be a feasible therapeutic approach for RTT, at least for the purpose of mitigating breathing abnormalities, a major morbidity.

In conclusion, the data reported here show a reduced GABAergic synaptic receptor-mediated phasic transmission and an increased GABAergic extrasynaptic transmission. This study demonstrates an imbalance in NTS GABA transmission that could provide a target for respiratory dysfunction in RTT.

Conflict of interest

The authors declare no competing financial interests.

Author contributions

C-Y.C., L-W.J., M.R., C-C.L. and I.M. designed the study and wrote the manuscript. J.DL and Y-C.L. performed the experiments and data analysis. All authors reviewed the manuscript.

Acknowledgments

References

Abdala, A.P., Dutschmann, M., Bissonnette, J.M., Paton, J.F., 2010. Correction of respiratory disorders in a mouse model of Rett syndrome. Proc. Natl. Acad. Sci. U. S. A. 107, 18208–18213.

Abdala, A.P., Toward, M.A., Dutschmann, M., Bissonnette, J.M., Paton, J.F., 2016. Deficiency of GABAergic synaptic inhibition in the Kolliker-Fuse area underlies respiratory dysrhythmia in a mouse model of Rett syndrome. J. Physiol. 594, 223–237.

Andresen, M.C., Kunze, D.L., 1994. Nucleus tractus solitarius—gateway to neural circulatory control. Annu. Rev. Physiol. 56, 93–116.

Banerjee, A., Rikhye, R.V., Breton-Provencher, V., Tang, X., Li, C., Li, K., Runyan, C.A., Fu, Z., Jaenisch, R., Sur, M., 2016. Jointly reduced inhibition and excitation underlies circuit-wide changes in cortical processing in Rett syndrome. Proc. Natl. Acad. Sci. U. S. A. 113, E7287–E7296.

Bittolo, T., Raminelli, C.A., Deiana, C., Baj, G., Vaghi, V., Ferrazzo, S., Bernareggi, A., Tongiorgi, E., 2016. Pharmacological treatment with mirtazapine rescues cortical atrophy and respiratory deficits in MeCP2 null mice. Sci Rep 6, 19796.

Bonham, A.C., 1995. Neurotransmitters in the CNS control of breathing. Respir. Physiol. 101, 219–230.

Bonham, A.C., Chen, C.Y., Sekizawa, S., Joad, J.P., 2006a. Plasticity in the nucleus tractus solitarius and its influence on lung and airway reflexes. J. Appl. Physiol. 101, 322–327.

Bonham, A.C., Sekizawa, S., Chen, C.Y., Joad, J.P., 2006b. Plasticity of brainstem mechanisms of cough. Respir. Physiol. Neurobiol. 152, 312–319.

Brickley, S.G., Mody, I., 2012. Extrasynaptic GABA(A) receptors: their function in the CNS and implications for disease. Neuron 73, 23–34.

Burton, M.D., Kazemi, H., 2000. Neurotransmitters in central respiratory control. Respir. Physiol. 122, 111–121.

Chahrour, M., Zoghbi, H.Y., 2007. The story of Rett syndrome: from clinic to neurobiology. Neuron 56, 422–437.

Chao, H.T., Zoghbi, H.Y., Rosenmund, C., 2007. MeCP2 controls excitatory synaptic strength by regulating glutamatergic synapse number. Neuron 56, 58–65.

Chao, H.T., Chen, H., Samaco, R.C., Xue, M., Chahrour, M., Yoo, J., Neul, J.L., Gong, S., Lu, H.C., Heintz, N., Ekker, M., Rubenstein, J.L., Noebels, J.L., Rosenmund, C., Zoghbi, H.Y., 2010. Dysfunction in GABA signalling mediates autism-like stereotypies and Rett syndrome phenotypes. Nature 468, 263–269.

Chen, C.Y., Bonham, A.C., 2005. Glutamate suppresses GABA release via presynaptic metabotropic glutamate receptors at baroreceptor neurones in rats. J. Physiol. 562, 535–551.

Chen, R.Z., Akbarian, S., Tudor, M., Jaenisch, R., 2001. Deficiency of methyl-CpG binding protein-2 in CNS neurons results in a Rett-like phenotype in mice. Nat. Genet. 27, 327–331.

Chen, C.Y., Bechtold, A.G., Tabor, J., Bonham, A.C., 2009. Exercise reduces GABA synaptic input onto nucleus tractus solitarii baroreceptor second-order neurons via NK1 receptor internalization in spontaneously hypertensive rats. J. Neurosci. 29, 2754–2761.

Dani, V.S., Chang, Q., Maffei, A., Turrigiano, G.G., Jaenisch, R., Nelson, S.B., 2005. Reduced cortical activity due to a shift in the balance between excitation and inhibition in a mouse model of Rett syndrome. Proc. Natl. Acad. Sci. U. S. A. 102, 12560–12565.

Ellaway, C., Christodoulou, J., 1999. Rett syndrome: clinical update and review of recent genetic advances. J. Paediatr. Child Health 35, 419–426.

Farrant, M., Nusser, Z., 2005. Variations on an inhibitory theme: phasic and tonic activation of GABA(A) receptors. Nat. Rev. Neurosci. 6, 215–229.

Gonzales, M.L., LaSalle, J.M., 2010. The role of MeCP2 in brain development and neurodevelopmental disorders. Curr. Psychiatry Rep. 12, 127–134.

Guy, J., Hendrich, B., Holmes, M., Martin, J.E., Bird, A., 2001. A mouse Mecp2-null mutation causes neurological symptoms that mimic Rett syndrome. Nat. Genet. 27, 322–326.

Huang, T.W., Kochukov, M.Y., Ward, C.S., Merritt, J., Thomas, K., Nguyen, T., Arenkiel, B.R., Neul, J.L., 2016. Progressive changes in a distributed neural circuit underlie breathing abnormalities in mice lacking MeCP2. J. Neurosci. 36, 5572–5586.

Jin, X., Cui, N., Zhong, W., Jin, X.T., Jiang, C., 2013. GABAergic synaptic inputs of locus coeruleus neurons in wild-type and Mecp2-null mice. Am. J. Physiol. Cell Physiol. 304, C844–857.

Joad, J.P., Munch, P.A., Bric, J.M., Evans, S.J., Pinkerton, K.E., Chen, C.Y., Bonham, A.C., 2004. Passive smoke effects on cough and airways in young guinea pigs: role of brainstem substance P. Am. J. Respir. Crit. Care Med. 169, 499–504.

Katz, D.M., Dutschmann, M., Ramirez, J.M., Hilaire, G., 2009. Breathing disorders in Rett syndrome: progressive neurochemical dysfunction in the respiratory network after birth. Respir. Physiol. Neurobiol. 168, 101–108.

Kline, D.D., Ogier, M., Kunze, D.L., Katz, D.M., 2010. Exogenous brain-derived neurotrophic factor rescues synaptic dysfunction in Mecp2-null mice. J. Neurosci. 30, 5303–5310.

Levitt, P., Campbell, D.B., 2009. The genetic and neurobiologic compass points toward

common signaling dysfunctions in autism spectrum disorders. J. Clin. Invest. 119, 747–754.

Livak, K.J, Schmittgen, T.D., 2001. Analysis of relative gene expression data using real-time quantitative PCR and the 2(-Delta Delta C(T)) method. Methods 25, 402–408.

Medrihan, L., Tantalaki, E., Aramuni, G., Sargsyan, V., Dudanova, I., Missler, M., Zhang, W., 2008. Early defects of GABAergic synapses in the brain stem of a MeCP2 mouse model of Rett syndrome. J. Neurophysiol. 99, 112–121.

Meng, X.L., Wang, W., Lu, H., He, L.J., Chen, W., Chao, E.S., Fiorotto, M.L., Tang, B., Herrera, J.A., Seymour, M.L., Neul, J.L., Pereira, F.A., Tang, J.R., Xue, M.S., Zoghbi, H.Y., 2016. Manipulations of MeCP2 in glutamatergic neurons highlight their contributions to Rett and other neurological disorders. elife 5.

Nusser, Z., Sieghart, W., Somogyi, P., 1998. Segregation of different GABAA receptors to synaptic and extrasynaptic membranes of cerebellar granule cells. J. Neurosci. 18, 1693–1703.

Pohodich, A.E., Zoghbi, H.Y., 2015. Rett syndrome: disruption of epigenetic control of postnatal neurological functions. Hum. Mol. Genet. 24, R10–16.

Sekizawa, S.I., Horowitz, J.M., Horwitz, B.A., Chen, C.Y., 2012. Realignment of signal processing within a sensory brainstem nucleus as brain temperature declines in the Syrian hamster, a hibernating species. J. Comp. Physiol. A. 198, 267–282.

Sekizawa, S.I., Horwitz, B.A., Horowitz, J.M., Chen, C.Y., 2013. Protection of signal processing at low temperature in baroreceptive neurons in the nucleus tractus solitarius of Syrian hamsters, a hibernating species. Am. J. Physiol.-Reg I 305, R1153–R1162.

Ure, K., Lui, H., Wang, W., Ito-Ishida, A., Wu, Z.Y., He, L.J., Sztainberg, Y., Chen, W., Tang, J.R., Zoghbi, H.Y., 2016. Restoration of Mecp2 expression in GABAergic neurons is sufficient to rescue multiple disease features in a mouse model of Rett syndrome. elife 5.

Voituron, N., Hilaire, G., 2011. The benzodiazepine midazolam mitigates the breathing defects of Mecp2-deficient mice. Respir. Physiol. Neurobiol. 177, 56–60.

Wasserman, A.M., Ferreira Jr., M., Sahibzada, N., Hernandez, Y.M., Gillis, R.A., 2002. GABA-mediated neurotransmission in the ventrolateral NTS plays a role in respiratory regulation in the rat. Am. J. Physiol. Regul. Integr. Comp. Physiol. 283, R1423–1441.

Zhang, L., He, J., Jugloff, D.G., Eubanks, J.H., 2008. The MeCP2-null mouse hippocampus displays altered basal inhibitory rhythms and is prone to hyperexcitability. Hippocampus 18, 294–309.

Zhong, W., Cui, N., Jin, X., Oginsky, M.F., Wu, Y., Zhang, S., Bondy, B., Johnson, C.M., Jiang, C., 2015. Methyl CpG binding protein 2 gene disruption augments tonic currents of gamma-aminobutyric acid receptors in locus coeruleus neurons: impact on neuronal excitability and breathing. J. Biol. Chem. 290, 18400–18411.

Zhong, W., Johnson, C.M., Wu, Y., Cui, N., Xing, H., Zhang, S., Jiang, C., 2016. Effects of early-life exposure to THIP on phenotype development in a mouse model of Rett syndrome. J. Neurodev. Disord. 8, 37.